remote sensing

MDPI

Article

Glacier Mass Balance Pattern and Its Variation Mechanism in the West Kunlun Mountains in Tibetan Plateau

Le Gao [1,2], Xiaofeng Yang [3,*], Jifeng Qi [1,2] and Wenfeng Chen [4]

1 CAS Key Laboratary of Ocean Circulation and Waves, Institute of Oceanology, Chinese Academy of Sciences and Center for Ocean Mega-Science, Chinese Academy of Sciences, No. 7 Nanhai Road, Qingdao 266071, China; gaole@qdio.ac.cn (L.G.); jfqi@qdio.ac.cn (J.Q.)
2 Pilot National Laboratory for Marine Science and Technology (Qingdao), No. 1 Wenhai Road, Qingdao 266237, China
3 State Key Laboratory of Remote Sensing Science, Aerospace Information Research Institute, Chinese Academy of Sciences, Beijing 100101, China
4 State Key Laboratory of Tibetan Plateau Earth System, Resources and Environment, Institute of Tibetan Plateau Research, Chinese Academy of Sciences, Beijing 100101, China; chenwf@itpcas.ac.cn
* Correspondence: yangxf@radi.ac.cn; Tel.: +86-010-6480-6215

Abstract: Mass balance observations are beneficial for assessing climate change in different world regions. This study analyzed the glacier elevation change, ice flux divergence, and surface mass balance (SMB) in the West Kunlun Mountains (WKM) on the Tibetan Plateau using remote sensing data, including satellite altimetry, glacier surface velocity, and thickness fields. Seventeen local glaciers were examined in detail and showed varying surface elevation changes from -0.39 ± 0.11 to 0.83 ± 0.10 m/a. Overall, we obtained a reasonably rapid elevation trend of 0.21 ± 0.14 m/a. By combining the ice flux divergence and surface mass balance, the overall thickness change of the WKM glacier over time is almost zero, and the WKM glacier shows a positive mass balance of 0.21 ± 0.98 m/a. Moreover, the ice flux divergence is more significant on the ice tongue than in the flat region due to the more considerable gradient of surface velocity and thickness fields. We found that glacier heterogeneity dynamics were associated with a surging dynamic mechanism concentrated in the glacier tongue and were induced by inner terrain instabilities. The glacier surging causes a drastic drop in glacier elevation but does not cause a glacier mass gain or loss, and it has an enhanced effect on the ice flux divergence. Therefore, glacier surging is the main reason for the decline of the two glaciers monitored. In addition, the long-term meteorological data analysis found that, since 2000, the air temperature warming hiatus may have balanced the three glaciers, and significantly increasing precipitation variation may cause the glacier to thicken the most.

Keywords: satellite altimetry; glacier elevation change; glacier inner terrain; glacier surging; ice flux divergence; surface mass balance; climate change

Citation: Gao, L.; Yang, X.; Qi, J.; Chen, W. Glacier Mass Balance Pattern and Its Variation Mechanism in the West Kunlun Mountains in Tibetan Plateau. *Remote Sens.* **2022**, *14*, 2634. https://doi.org/10.3390/rs14112634

Academic Editor: Gareth Rees

Received: 3 April 2022
Accepted: 30 May 2022
Published: 31 May 2022

1. Introduction

Mountain glaciers are not only an important indicator of climate change, but also major contributors to sea level rise and water resources in many downstream areas [1,2]. Since the 1970s, satellite altimetry has been applied to monitor the elevation changes of the ice sheets covering the two poles and Greenland [3,4]. However, the footprint of microwave radar altimeters, e.g., Envisat and Jason-1/2 satellites, reaches ~2 km in diameter. The accuracy of elevation observations in mountain areas is affected considerably by the complex terrain. This means that it is difficult to use microwave radar altimeters to monitor the typical mountain glacier. Fortunately, the spatial resolution of the Ice, Cloud and land Elevation Satellite (ICESat) Geoscience Laser Altimeter System (GLAS) elevation datasets is very high, and the footprint diameter is only 70 m and the distance between adjacent along-track footprints is only 170 m. More importantly, ICESat elevation data have high vertical

accuracy in mountain areas [5]. Therefore, ICESat elevation data provide the opportunity to monitor glacier elevation changes in rugged terrain [6–8].

According to previous studies of glacier mass and area, most glaciers across the Qinghai–Tibetan Plateau (QTP) are thinning, losing mass, and retreating. Moreover, the ablation rate has been projected to increase to a serious degree by 2100 [9,10]. However, glacier mass changes are not uniform and they show contrasting patterns in different local areas. For example, the Eastern Himalaya region has reported the greatest rate of mass loss (−0.6 m/a) and the Central Himalaya area had moderate mass loss (−0.4 m/a). In contrast, the mass of the glaciers in the Western Kunlun and parts of the Karakoram and Eastern Pamir regions has shown a trend of balance or even slight increase. This mass balance anomaly has received considerable attention and research in atmospheric circulation mode over East Asia [9–12]. Individual glaciers in regions/subregions also show a distinctive heterogeneous pattern. Heterogeneous glacier changes are observed not only in terms of the changes in their length and area, but also in the spatial distribution of surface elevation changes [12]. According to the China Glacier Inventory [13,14], the WKM region has the largest concentration of contemporary large mountain glaciers. The absence of information on individual glacier changes leaves a gap in the understanding of the local glacier dynamics and driving factors, which could affect the quantitative assessment of the overall glacier mass balance.

The glacier surface mass balance (SMB) is determined by the process of mass gain or mass loss, which is affected by factors such as the energy budget, snowfall, freezing rain, snow and ice melt, sublimation, and precipitation over the glacier. Because of the direct link with local climate signals, it is important to determine the SMB and its distribution. Previous studies have attempted to determine SMB over one period by implementing mass continuity or 3D ice flow modeling based on the principle of combining surface elevation changes with the ice flux divergence, such as [15–18]. However, limited by the available measurements, the heterogeneity of the SMB cannot be captured sufficiently [19,20].

In this study, we focus on trends in glacier elevation, ice flux divergence, and SMB of individual glaciers using ICESat/GLAS elevation measurements, open-source thickness and velocity fields, and to explore the reasons for the heterogeneous pattern of glacier dynamics. In particular, internal terrain and surging are essential for understanding glacier glaciological processes and dynamics. Therefore, influencing factors on glacier elevation changes are discussed in detail.

2. Study Area and Data Used

2.1. Study Area

The inland mountain range of the WKM extends southward in an arc at the northwest edge of the QTP. The WKM glacier (35.19°–35.6°N, 80.29°–81.79°E) considered in this study covers an area of ~3307 km^2, shown in Figure 1. It is an area of continuous mountain glaciers with mean elevation of 6500 m and marked topographic relief. The studied area is a typical continental glacier area with features of polar glaciology. The complex terrain of the northern slopes is dominated by dendritic large valley glaciers, whereas the terrain of the southern slopes is comparatively smooth.

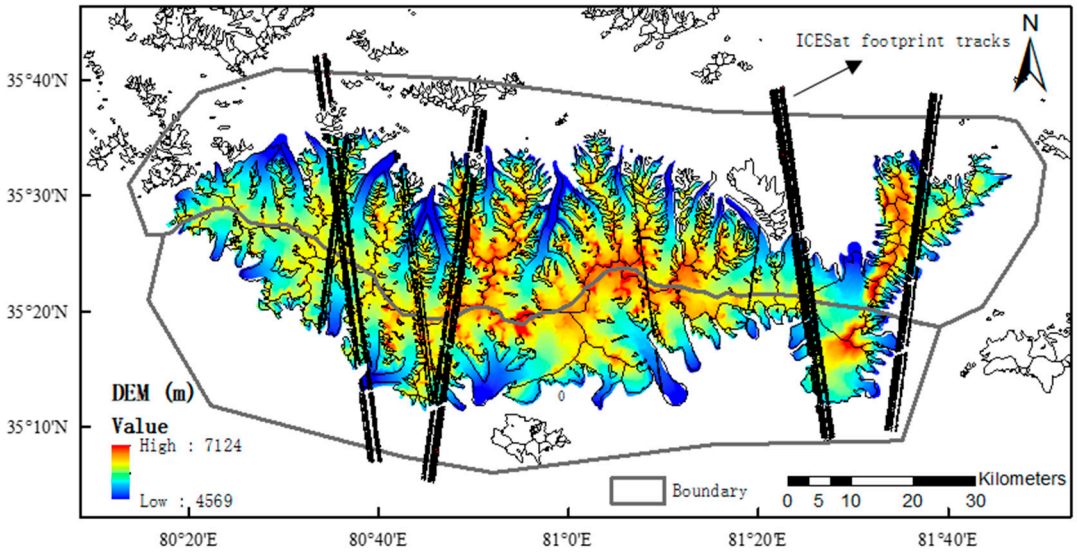

Figure 1. Study area: West Kunlun Mountains glaciers investigated in this study, SRTM-DEM elevations of the West Kunlun Mountains glacier obtained in 2000, and ICESat footprint coverage over glacier-covered and off-glacier areas within 15 km.

2.2. Data Used

2.2.1. ICESat/GLAS Altimeter Data

Because the accuracy of pulse-limited microwave altimeters (e.g., the Envisat and Jason-1/2 satellites) is poor on mountain glaciers, only the laser altimetry geophysical data record of ICESat/GLAS GLA14 Level 2 was used due to the only 70 m footprint diameter. The ICESat/GLAS altimeter uses a near-infrared (1064 nm) laser pulse to measure elevation over the along-track discrete footprint. Elevation data were collected every 3–6 months during 18 ICESat laser periods from February 2003 to November 2009. Because small quantities of available data could lead to biased sampling, the datasets from some tracks in 2003 and incomplete datasets from the 2009 campaign (2F) were excluded. The reference system of the ICESat/GLAS altimeter data is the Topex/Poseidon ellipsoid. To maintain consistency with the WGS84 reference system, the ICESat/GLAS elevations were converted to WGS84 ellipsoid elevations [21]. Although the new generation of the ICESat-2 satellite was launched in September 2018, there was a ten-year gap from 2009 to 2018, and so its data are not used due to the short data volume and time duration.

2.2.2. Digital Elevation Model

Digital elevation model (DEM) data are an important topographical reference when applying ICESat data in the estimation of elevation changes of mountain glaciers [7,22]. Because of the known time stamp of individual glacier elevation pixels, Shuttle Radar Topography Mission (SRTM) DEM data with 3-arcsec resolution were used to extract glacier elevation at points corresponding to ICESat footprints and topographic parameters of the glacier surface, including slope, aspect, and roughness (Figure 1). We performed the SRTM DEM co-registration and systematic penetration error correction using the method proposed by Wang et al. [23]. It is worth noting that the SRTM data were used to separate spatial variation in surface elevation from temporal variation and not as part of the time series analysis.

2.2.3. Second Glacier Inventory of China

The vector boundaries of the glaciers were used from the glacier inventory dataset. We used the Second Glacier Inventory of China as a mask to classify ICESat footprints into on-glacier and off-glacier points [24]. The off-glacier footprints were limited to within a 15 km buffer of the glacier outlines.

2.2.4. Glacier Surface Velocity and Thickness Fields

To estimate the ice flux divergence, this study used the depth-averaged global glacier flow datasets with the resolution of 240 m (annual average) provided by the NASA MEaSUREs project (https://its-live.jpl.nasa.gov/, accessed on 29 May 2022). In addition, Farinotti et al. [25] also reported global ice thickness products with the resolution of 25, 50, 100 or 200 m (https://doi.org/10.3929/ethz-b-000315707, accessed on 29 May 2022). We resampled both the velocity and thickness fields to 25 m resolution using the cubic spline interpolation method to unify the resolution and maintain data detail.

3. Methodology

3.1. Altimetry-Derived Glacier Surface Elevation Trends

Changes in glacier elevation were estimated by differencing DEMs at different times. The spatial scale of the individual local glacier is small, much less than <1° (Figure 1). Therefore, the elevation trend of all the observation points can characterize the local glacier changes at the 1° × 1° geographic grid [26,27], and we only use the along-track ICESat observations on each local glacier for trend estimation. In this study, we used the MATLAB function robustfit with default parameterization to estimate the glacier elevation difference (dh) changes. This regression method uses an iterative reweighted least squares approach, where all dh data points are given equal weighting for the first iteration, while, in subsequent iterations, the weights of the points furthest from the regression model are decreased, until the regression coefficients converge to a constant value. The dh trend represents the mean change in elevation difference over the ICESat acquisition period. To avoid the influence of seasonal snowfall on the trend of on-glacier dh values, the dh data obtained in autumn (October–December) and winter (February–April) were used to estimate the interannual elevation trends. Moreover, the equilibrium line of the glacier is a set of points on the surface where the climatic mass balance is zero. The equilibrium line separates the accumulation area (where the glacier is gaining mass in general) from the ablation area (where the glacier is losing mass). According to recent studies [9,10,27,28], the equilibrium line altitude (ELA) in recent years has shown a trend of increase because of climatic variability and other factors, and the mean ELA was around 5930 m. Some glaciers only had ICESat measurements over several separate accumulation or ablation areas. For these cases, the dh trends were calculated separately for the different accumulation/ablation areas as long as the coverage of ICESat measurements was sufficient. For a better visual representation, dh medians of Guliya and Zhongfeng glacier in each laser period are shown in Figure 2.

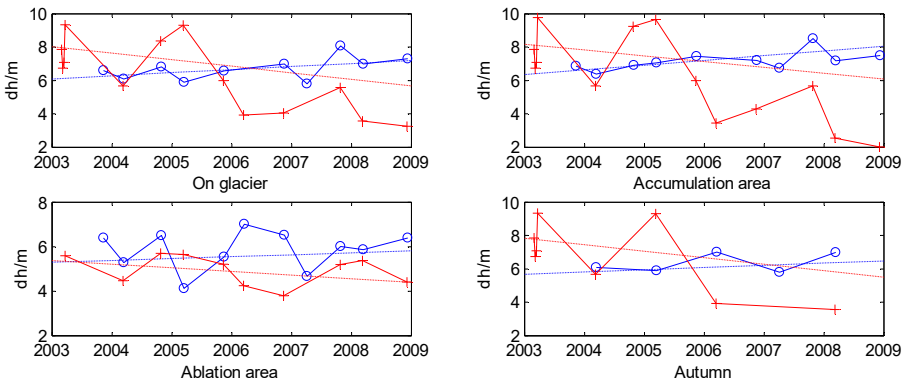

Figure 2. *Cont.*

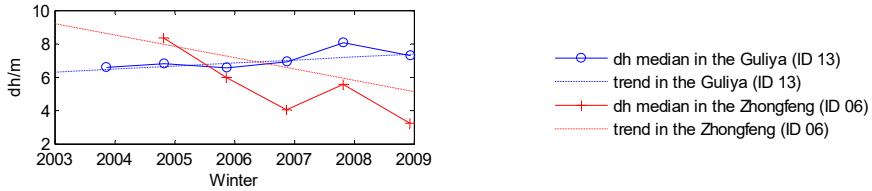

Figure 2. Glacier elevation changes derived from the elevation difference (dh) values between ICESat and SRTM for the Guliya and Zhongfeng glaciers. For a better visual representation, median dh values in each laser period are shown. Trends were fit through all dh values in autumn and winter seasons.

3.2. ICE Flux Divergence and Glacier Mass Balance

The ice flux divergence represents the upward or downward flow of ice relative to the glacier surface and determines the rate of temporal change of its thickness. This flow compensates for the SMB exactly if the glacier is under steady state conditions. Ice flux divergence sometimes is called emergence or submergence velocity and represents the difference between the ice supplied from upstream and lost downstream at a particular position. When ice mass is supplied to the surface, it is defined as negative and called the emergence velocity. When ice mass is removed from the surface, it is defined as positive for downward motion and referred to as the submergence velocity. Van Tricht et al. [20] reported the ice flux divergence as a function of ice thickness and surface velocities, shown in Equation (1):

$$\nabla \cdot \vec{q} = F(u_{s,x}\frac{\partial H}{\partial x} + u_{s,y}\frac{\partial H}{\partial y} + H\frac{u_{s,x}}{\partial x} + H\frac{u_{s,x}}{\partial y}) \quad (1)$$

where F is the depth-averaged glacier velocity ratio (here, it is 0.9), u_s is the glacier surface velocities; H is the glacier thickness; $\frac{\partial H}{\partial x}$, $\frac{\partial H}{\partial y}$, $\frac{u_{s,x}}{\partial x}$ and $\frac{u_{s,x}}{\partial y}$ are the gradients of glacier thickness and surface velocity in the x and y directions.

The ice flux divergence also explains the change in ice thickness over time. Therefore, the SMB can be estimated by the sum of the ice elevation changes and ice flux divergence using Equation (2):

$$b_s = \frac{\partial h}{\partial t} + \nabla \cdot \vec{q} \quad (2)$$

where b_s is the SMB, and $\frac{\partial h}{\partial t}$ is the glacier elevation change obtained from ICESat altimetry data.

4. Results

4.1. Elevation Changes

We obtained surface elevation changes for 17 local glaciers sampled along repeated ICESat tracks. Table 1, Figures 3 and 4 reveal that the WKM glaciers are characterized by heterogeneous behavior of surface elevation change during 2003–2008, with trends ranging from -0.39 ± 0.11 m/a (Zhongfeng glacier, ID 6) to 0.83 ± 0.10 m/a (5Y641F0046, ID 14). Jansson [29] suggests that the glacier mass balance is uncertain by approximately 0.1 m/a. Therefore, we use ± 0.1 m/a as a balance criterion. For on-glacier changes, twelve glaciers (70.59%) show increasing trends of surface elevation (trends > 0.1 m/a), while three glaciers (17.65%) are in balance (trends within ± 0.1 m/a). The two remaining glaciers (11.76%, Zhongfeng glacier and 5Y641F0049) show significant thinning trends (trends < -0.1 m/a). Overall, the trend of surface elevation change for local glaciers is 0.21 ± 0.14 m/a during 2003–2008, which confirms the overall positive mass balance for WKM glaciers in previous studies [27,30]. The level of mass gain/loss varies across different glaciers, resulting in variability in the overall balance. In autumn/winter, the Zhongfeng (ID 6) and 5Y641F0049 (ID 11) glaciers are thinning, and other glaciers are thickening or in balance, ensuring that the entire WKM glaciers mainly belong to the thickening type. Elevation change trends over accumulation/ablation areas reveal varying mass budgets within different parts of the glaciers (Figure 4a,b). In accumulation areas (areas with an altitude of $\geq$5930 m), the mean trends range from -0.39 ± 0.11 m/a (Zhongfeng glacier,

ID 6) to 0.83 ± 0.10 m/a (5Y641F0046, ID 14). Thirteen glaciers (76.47%) show increasing trends, only one glacier (5.88%, Zhongfeng glacier, ID 6) shows a significant decreasing trend (−0.39 ± 0.11 m/a), and three glaciers (17.65%) are in balance (Figure 4a). Since some dh values were unavailable only in ablation areas, only 12 glaciers were monitored (Figure 4b and Table 1). Four glaciers (33.3%) show significant increasing trends, another four (33.3%) are in balance, and the remaining four glaciers (33.3%) show significant decreasing trends. Their mean trends range from −1.16 ± 0.75 m/a (Gongxing glacier, ID 4) to 1.32 ± 0.19 m/a (Duota glacier, ID 3). Previous studies also reported an increase in glacier elevation during 2003–2008, which is reasonably consistent with our results, shown in Table 2. However, we found that our result has some differences compared with previous studies and shows a more mixed picture. For example, Kääb et al. [26] reported a trend of 0.05 ± 0.07 m/a based on autumn ICESat acquisitions on the entire WKM glacier area. In contrast, the significant thickening trend of this study is 0.19 ± 0.17 m/a based on the mean of 17 glaciers (Table 1). The reason for this difference in results is that the ratio of glacier area covered by ICESat point measurements versus the total glacier area is only ~40.97%. Therefore, this shows the necessity for more detailed local glacier estimations. For off-glacier areas, the estimated trends are close to 0 m/a, meaning that the estimated trends of on-glacier areas are obtained fully from the glacier itself and also verify the credibility of estimating the change rate of glacier areas.

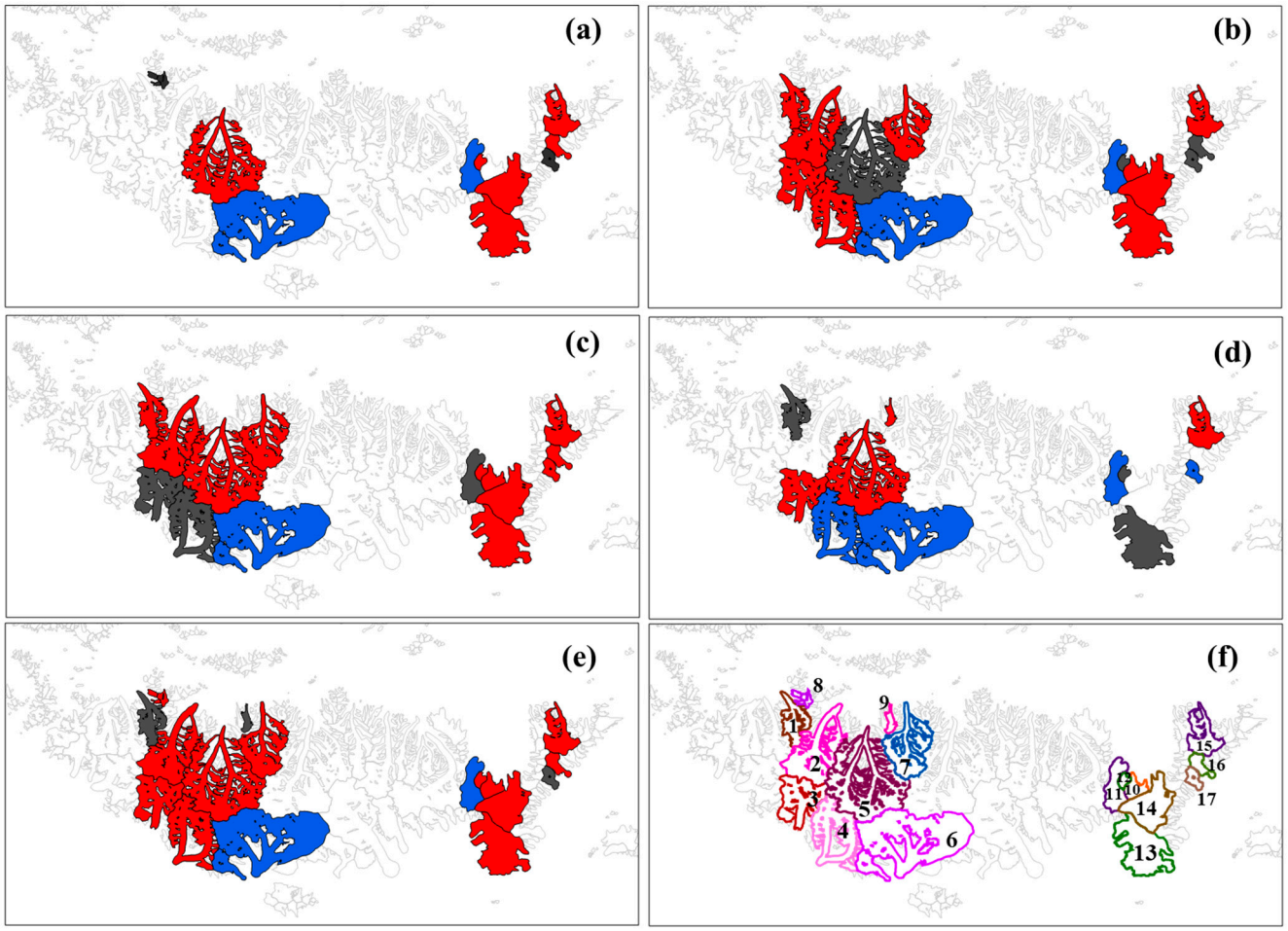

Figure 3. Trends of dh values between ICESat and SRTM during 2003–2008 for 17 local glaciers in the WKM region. Mean trends for individual glaciers are shown in different colors (red: thickening, blue: thinning, grey: in balance within ±0.1 m/a). (**a**) Winter, (**b**) autumn, (**c**) accumulation area, (**d**) ablation area, (**e**) on-glacier area, and (**f**) distribution of individual glaciers with ICESat measurements within the WKM region.

Table 1. Trends (m/a) of dh values for different parts of the glaciers and other general statistics.

Local Glacier ID	Glacier Name	Count of Footprints	dh Trend (m/a)						Glacier Area (km^2)	Mean Elevation (m a.s.l)	Mean Slope (degree)	Mean Aspect	Mean Roughness
			Winter	Autumn	Accumulation Area	Ablation Area	On-Glacier Area	Off-Glacier Area					
1	5Y641H0067	353	—	**0.15 ± 0.14**	**0.19 ± 0.10**	−0.07 ± 0.14	−0.05 ± 0.11	−0.03 ± 0.04	44.195	6049.8	8.2826	232.3274	1.0160
2	West Yulong 5Y641G0068	628	—	**0.28 ± 0.10**	**0.19 ± 0.09**	—	**0.20 ± 0.09**	−0.03 ± 0.04	120.5	6097.7	7.4202	120.5910	1.0154
3	Duota 5Z433C0020	458	—	**0.23 ± 0.11**	0.09 ± 0.12	**1.32 ± 0.19**	**0.31 ± 0.11**	−0.03 ± 0.04	80.996	6040.4	8.3379	192.9959	1.0185
4	Gongxing 5Z433C0027	381	—	0.26 ± 0.20	0.04 ± 0.16	−1.16 ± 0.75	0.23 ± 0.21	−0.03 ± 0.04	108.183	5972.2	10.8266	130.1602	1.0283
5	Kunlun 5Y641G0055	623	**0.34 ± 0.11**	**0.07 ± 0.16**	**0.27 ± 0.09**	0.24 ± 0.15	**0.35 ± 0.09**	−0.03 ± 0.04	199.088	6101.4	10.0992	193.6727	1.0242
6	Zhongfeng 5Z433D0008	706	**−0.68 ± 0.27**	**−0.39 ± 0.15**	**−0.35 ± 0.13**	−0.16 ± 0.17	**−0.39 ± 0.11**	−0.03 ± 0.04	237.458	6150.3	9.7051	145.5690	1.0242
7	5Y641G0038	206	—	0.26 ± 0.27	0.36 ± 0.20	—	**0.45 ± 0.19**	−0.03 ± 0.04	90.256	6152.2	11.1139	158.3028	1.0282
8 **	5Y641H0064, 65,66, and 5Y641G0088	119	0.01 ± 0.32	0.35 ± 0.24	0.12 ± 0.33	0.07 ± 0.20	0.23 ± 0.19	−0.03 ± 0.04	9.363	5935.2	13.8402	230.9515	1.0389
9	5Y641G0045	123	—	**0.66 ± 0.32**	0.40 ± 0.29	0.31 ± 0.42	**0.63 ± 0.25**	−0.03 ± 0.04	8.517	6018.8	14.9394	162.0498	1.0454
10 *	5Y641F0047	109	—	0.34 ± 0.22	0.28 ± 0.16	—	0.28 ± 0.16	0.04 ± 0.03	18.810	6047.6	11.3647	81.2169	1.0265
11	5Y641F0049	262	−0.17 ± 0.32	−0.21 ± 0.25	0.02 ± 0.18	−0.52 ± 0.11	−0.20 ± 0.19	0.04 ± 0.03	41.892	5838.5	6.5255	160.8932	1.0101
12	5Y641F0048	139	0.40 ± 0.26	0.02 ± 0.17	0.12 ± 0.22	0.05 ± 0.15	0.14 ± 0.15	0.04 ± 0.03	6.840	5872.8	9.5336	91.6888	1.0172
13	Guliya 5Z431C0022	732	0.13 ± 0.10	**0.18 ± 0.06**	**0.28 ± 0.06**	0.08 ± 0.10	**0.18 ± 0.06**	0.04 ± 0.03	111.371	5989.3	6.5990	245.4506	1.0102
14 *	5Y641F0046	163	**1.01 ± 0.19**	**0.75 ± 0.10**	**0.83 ± 0.10**	—	**0.83 ± 0.10**	0.04 ± 0.03	84.9704	6160.9	5.4266	115.4411	1.0065
15	5Y641F0023	506	**0.32 ± 0.14**	**0.29 ± 0.12**	0.11 ± 0.10	**0.63 ± 0.20**	**0.29 ± 0.09**	0.04 ± 0.03	50.92	5956.3	7.7895	125.7124	1.0151
16	5Y636J0100	210	0.25 ± 0.15	0.04 ± 0.16	0.15 ± 0.11	—	0.15 ± 0.11	0.04 ± 0.03	15.724	6122.0	7.5922	135.3	1.0143
17	5Y636J0098	148	0.04 ± 0.25	−0.05 ± 0.18	0.23 ± 0.14	−0.39 ± 0.31	−0.00 ± 0.15	0.04 ± 0.03	12.247	5953.8	9.5841	155.2660	1.0168
18	Overall ***	5866	0.17 ± 0.21	0.19 ± 0.17	0.20 ± 0.15	0.03 ± 0.24	0.21 ± 0.14	0.00 ± 0.04	1241.33	6027.01	9.3518	157.5053	1.0209

Bold numbers indicate that the trends are significant at the 95% significance level; * dh values only available in accumulation area; ** glacier ID 8 is a combination of three adjacent glaciers; *** overall results are estimated based on the mean of 17 local glaciers.

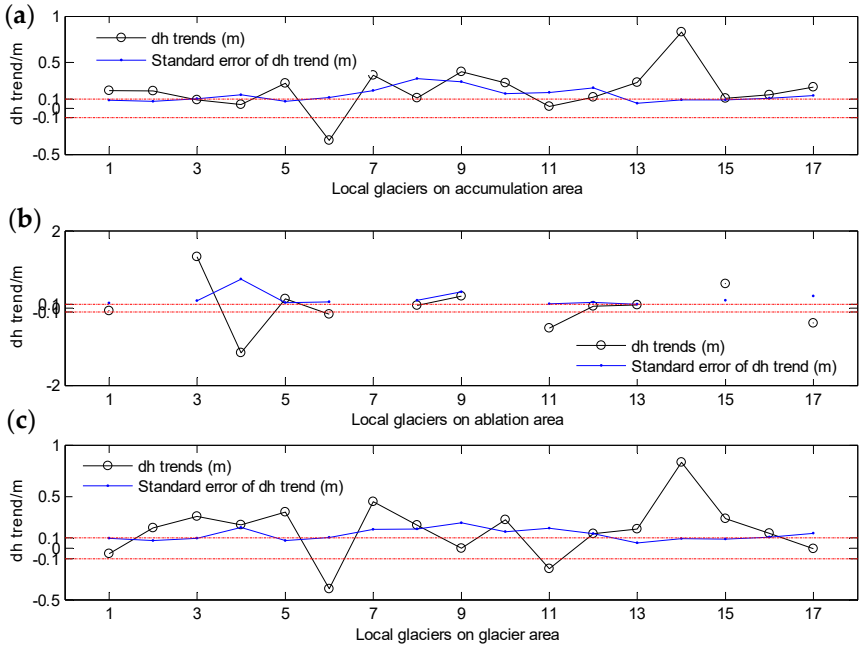

Figure 4. Glacier elevation change trends. (**a**) Accumulation area, (**b**) ablation area, and (**c**) on-glacier area.

Table 2. Comparison of glacier elevation change within the WKM region (m/a, ± at 1σ-level).

Data Source	Duration	On-Glacier	Accumulation Area	Ablation Area	Ref.
ICESat, SRTM	2003—2008	0.21 ± 0.14	0.20 ± 0.15	0.03 ± 0.24	This study
	2003—2009	0.17 ± 0.15	—	—	[8]
	2003—2008	—	—	0.04 ± 0.29	[22]
	2003—2009	0.22 ± 0.07	0.42 ± 0.09	0.01 ± 0.10	[30]
	2003—2008	0.20 ± 0.04	0.19 ± 0.05	0.22 ± 0.08	[27]
	2003—2008	0.05 ± 0.07	—	—	[26]

4.2. Glacier Velocity, Thickness, Flux Divergence, and Mass Balance

Figure 5a,b show that the average velocity of the entire WKM glacier is 3.16 ± 11.93 m/a, the average thickness is 57.36 ± 80.61 m, and the velocity above 150 m/a (a key indicator of surging, [31]) and the greater glacier thickness are mainly concentrated in the ice tongues. Neglecting temporal changes in thickness and thickness gradient and assuming that surface velocities are close to depth averaged velocities, we obtained the ice flux divergence of the entire WKM glacier using the glacier flow datasets provided by the NASA MEaSUREs project and ice thickness products provided by Farinotti et al. [25] in the WKM region based on Equation (1). Figure 5c shows that WKM glaciers had a velocity of 0.00 ± 0.97 m/a, i.e., the ice thickness change over time was almost zero. Therefore, for the 17 local glaciers, the estimated SMB is 0.21 ± 0.98 m/a because of the ICESat-based surface elevation (or thickness) change of 0.21 ± 0.14 m/a and ice flux divergence of 0.00 ± 0.97 m/a using Equation (2).

Figure 6 is the so-called "quiescent-state" of the Guliya glacier. Its averaged velocity is 3.76 ± 5.94 m/a (Figure 6a), the averaged thickness is 66.90 ± 78.54 m (Figure 6b), and the estimated ice flux divergence of the entire Guliya glacier is 0.00 ± 0.41 m/a (Figure 6c,d), showing that the change in the entire Guliya glacier's thickness with time is almost zero. In contrast, it had a tiny negative emergence velocity of −0.02 ± 0.47 m/a for the area of the ICESat footprints (Figure 6c,d). Therefore, we found that the ice flux divergence of the ICESat footprint area was almost consistent with the entire Guliya result. Furthermore, by Equation (2), the SMB of 0.16 ± 0.48 m/a can be obtained from the ICESat-based elevation

change of 0.18 ± 0.06 m/a and ice flux divergence of -0.02 ± 0.47 m/a, which indicated that the Guliya glacier exhibits a weak positive mass balance.

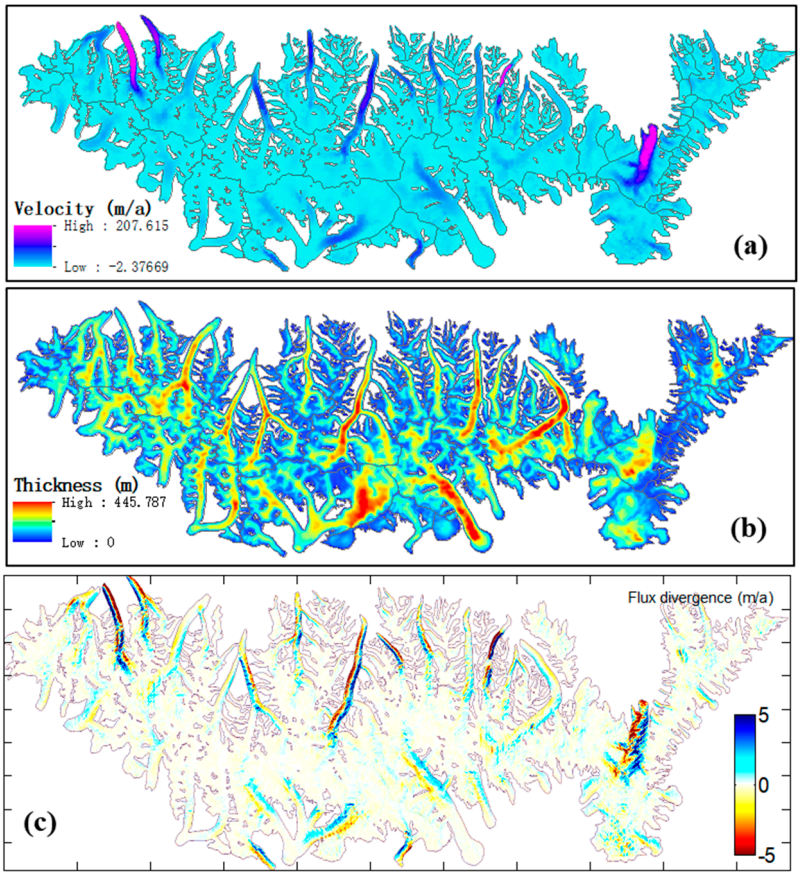

Figure 5. Ice velocity (**a**), thickness (**b**), and ice flux divergence (**c**) of WKM glacier.

From the above typical glaciers, we can determine that the uncertainty of the ice flux divergence is mainly derived from the accuracy of the glacier velocity and thickness fields [32]. For example, on the WKM glacier, Millan et al. [33] also provided the glacier thickness fields and showed a specific difference from Farinotti et al. [25] (thickness ranges: 0.00–417.40 m vs. 8.49–998.76 m). The accuracy of each SMB is limited by the overall distribution of the sparse ICESat footprints in the entire glacier. Nonetheless, such sparse ICESat altimetry data provided the possibility to evaluate many glaciers in remote areas. This was unimaginable before the appearance of the ICESat satellite.

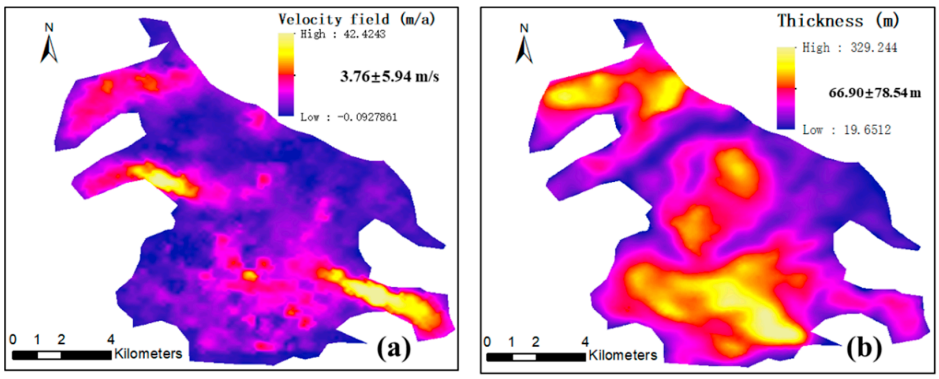

Figure 6. *Cont.*

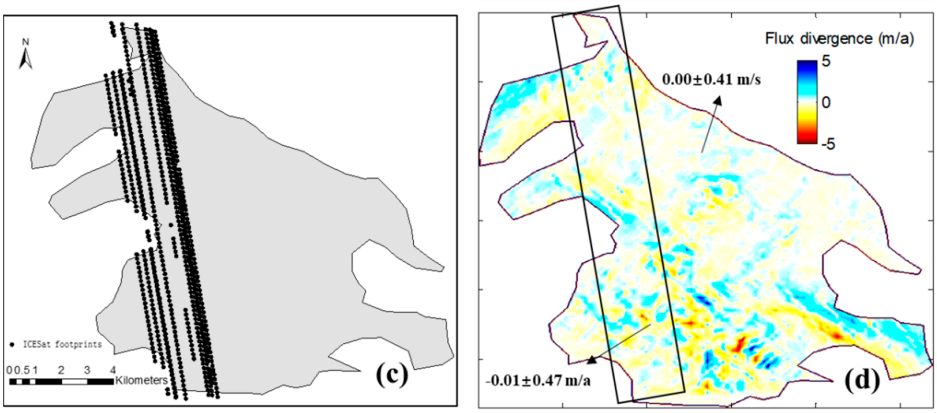

Figure 6. Velocity (**a**), thickness (**b**), ICESat footprints' coverage area (**c**), and ice flux divergence (**d**) of Guliya glacier.

5. Discussion

5.1. Glacier Surging

The analyses of glacier changes should distinguish carefully between surging and non-surging glaciers, because surging glaciers exhibit patterns of elevation change inconsistent with those of nearby non-surging glaciers. The phenomenon of glacier surging refers to the faster advance of a glacier tongue in comparison with normal conditions, or the elevation changes rapidly within a few days or up to 2–3 years. Li et al. [34] reported the surge occurrence of the Zhongfeng glacier (ID 6) in the WKM region by areal changes visible in Landsat imagery acquired during 2002–2004. In this study, an abnormal elevation change was also observed in the accumulation area of the Zhongfeng glacier (Figure 7a). From the latitudinal profiles of ICESat measurements over the Zhongfeng glacier, a drastic drop in dh values was found in each laser period from 2003 to 2008 (Figure 7b). This drastic surface lowering is a typical feature of glacier surging, and it is associated with rapid ice mass transport from upstream to downstream areas when the surging occurred [31]. The drastic drop in dh values also clearly distinguishes measurements made before (2003–2004), during (2004–2005), and after the surge (2006–2008). Moreover, when the glacier surge occurs, glacier mass in a high-altitude zone (i.e., accumulation zone) rapidly is transported to a low-altitude zone (i.e., ablation zone, Figure 7a). Therefore, glacier surging results in thinning in high-altitude regions and thickening in low-altitude regions, and there is no gain or loss of ice mass. Furthermore, from the elevation change profile, we can accurately find the surging location and direction to support disaster relief, shown as the light red box in Figure 7a. As a control and reference group for surging glaciers, the Guliya glacier (ID 13, Figure 6) is a typical example of a non-surging glacier. Although the elevation changes of the Guliya and Zhongfeng glaciers are broadly similar, there is an abnormal opposite phase during 2005–2006/2006–2007 (Figure 2). Glacier thickening might be related primarily to increased precipitation [35].

Figure 8 shows that the averaged velocity of the surging Zhongfeng glacier is 0.61 ± 6.41 m/a (Figure 8a), the averaged thickness is 82.45 ± 99.073 m (Figure 8b), and the overall averaged ice flux divergence is also 0.00 ± 0.56 m/a (Figure 8c), also showing that the change in the glacier thickness with time is almost zero. However, at the location of the ice tongue of the "surging" occurrence (in the black box), the ice flux divergence was significant at 0.29 ± 0.74 m/a (Figure 8d). By comparing the velocity fields in different years (Figure 8e), we found that the average velocity field is smaller than the individual annual average velocity field from 2003 to 2008. In particular, the velocity in 2006 was the largest. It corresponds to a significant ice flux divergence (submergence velocity) of 0.72 ± 3.68 m/a, which shows that the surging effect has also a significant enhancement effect on the ice flux divergence. At the same time, we also found that the ice flux divergence had a significant standard deviation, mainly caused by the large velocity field error in 2006. The SMB of -0.10 ± 0.75 m/a can be obtained from the ICESat-based elevation change of

-0.39 ± 0.11 m/a and ice flux divergence of 0.29 ± 0.74 m/a in the footprint area. This showed that the Zhongfeng glacier presented a negative mass balance.

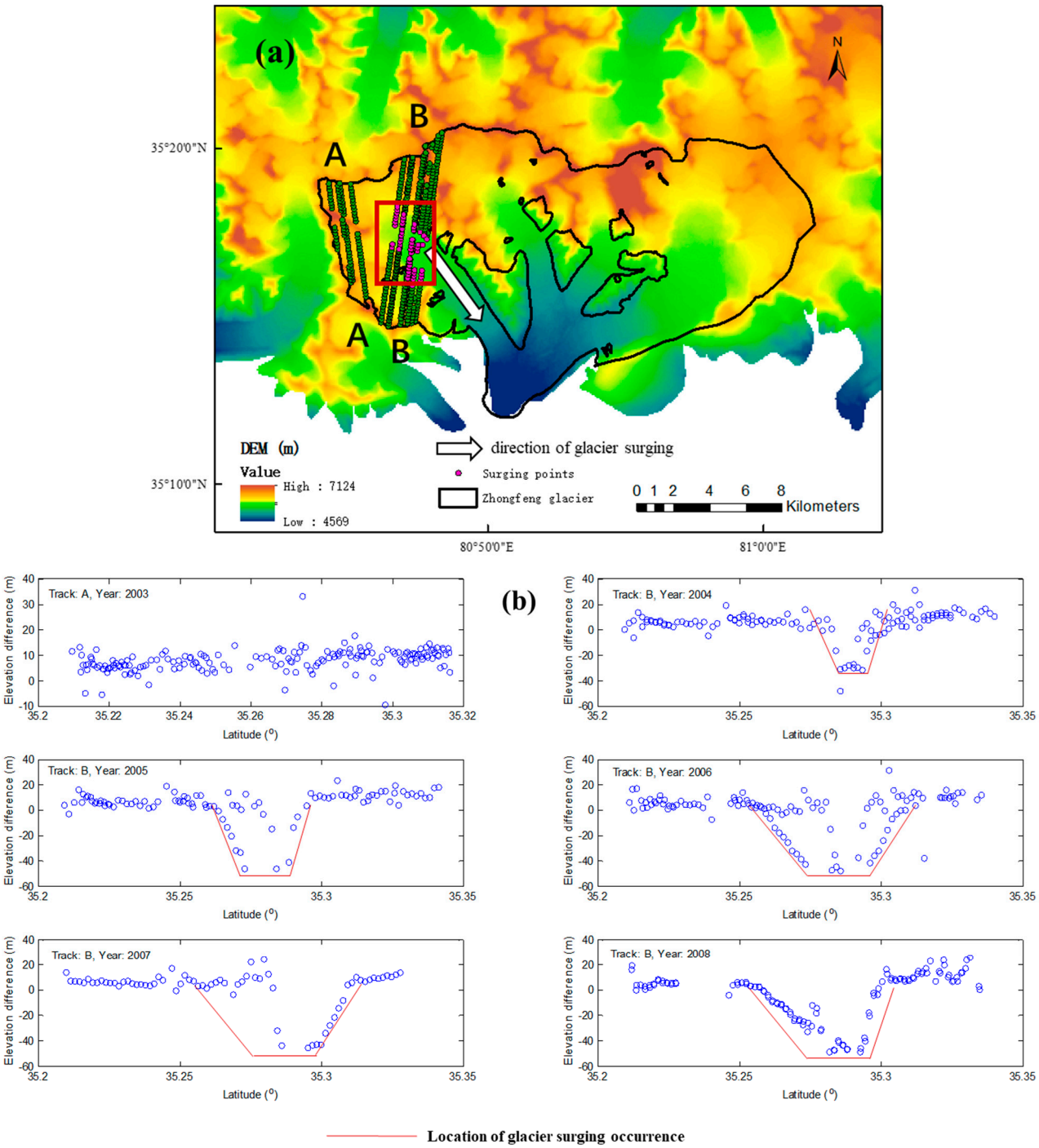

Figure 7. Surging Zhongfeng glacier laser coverage location and elevation time series. (**a**) ICESat data distribution over the accumulation area of Zhongfeng glacier; (**b**) drastic drop in elevation difference along the latitudinal profiles on Zhongfeng glacier.

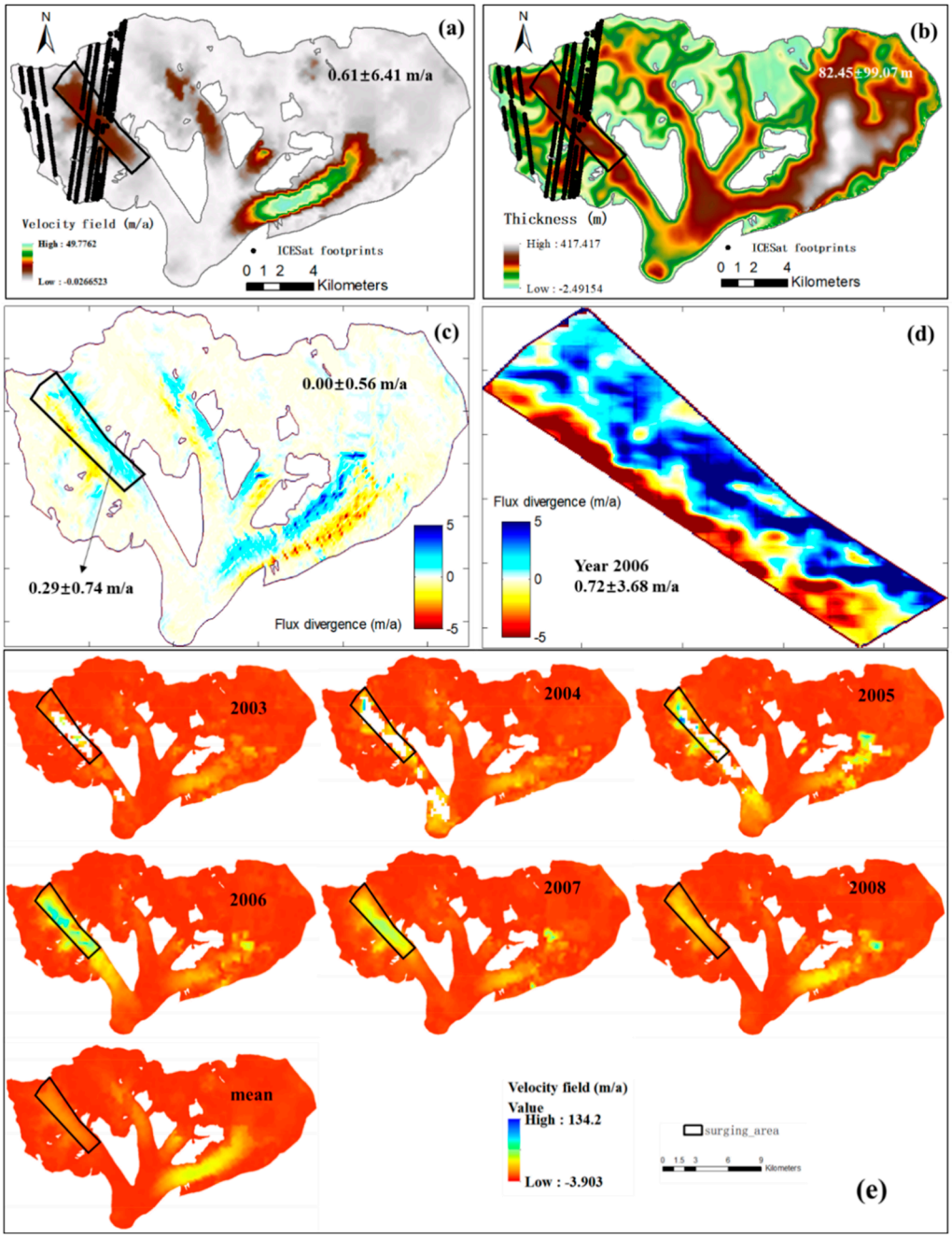

Figure 8. Glacier velocity (**a**), thickness (**b**), and flux divergence (**c**,**d**), and surface velocity field time series (**e**) of Zhongfeng glacier.

Glacier surging is more likely caused by internal instabilities. The topographical physical parameters are obtained from the average of SRTM DEMs corresponding to all ICESat footprints on the individual local glaciers. To reduce the influence of altitude on glacier change, 12 local glaciers within the same altitude range (5930–6150 m) were selected to discuss the relationship between glacier elevation change (or SMB) and other terrain factors (Figure 9). The correlation coefficients of "roughness" and "surface slope" with the elevation difference trend are 0.566 and 0.660, respectively. They indicate that the glacier's topography correlates relatively highly with the elevation difference trend. In addition, Figure 9 also shows the effect of topography-induced internal glacier instability on glacier thickness variation. For the surface slope, it is an essential factor affecting glacier surging. Figure 9a shows that higher slopes tend to have higher melting trends;

the surface aspect represents the glacier's attitude toward the sun, affecting the glacier's sunshine duration and evaporation intensity. For the Zhongfeng glacier, the mean slope of the glacier surface reached 9.71° (0.64–29.94°). The large slope might be an indicator of a significant terminus advance. Figure 9b shows that the mean elevation trends in the south slope were higher than that in the north sectors; under more similar terrain conditions (e.g., altitude range: 5956.3–6097.7 m, slope range: 7.4202–7.7895°, aspect range: 120.5910–125.7124°, and roughness range: 1.0151–1.0154), the dh trends of glaciers ID 2 and ID 15 are 0.20 ± 0.09 and 0.29 ± 0.09 m/a, respectively, indicating that eastern glaciers might have more significant trends of thickening than western glaciers. The "roughness" characterizes the smoothness of the terrain on which the local glacier is located, and it is another possible factor affecting glacier surging. Figure 9c shows that glaciers tend to have higher decreasing trends as roughness increases. Therefore, the inner terrain dependence may partly explain the spatial variability of glacier surging in the WKM region. Thus, we infer that unstable internal topography causes glacier surging, and glacier surging causes a rapid anomalous morphology of glacier variation.

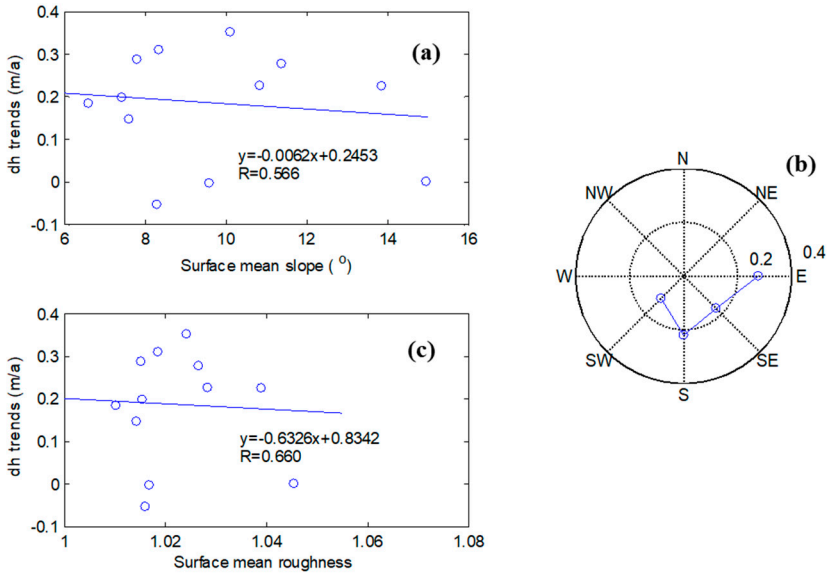

Figure 9. Trends of individual glaciers versus mean (**a**) slope, (**b**) aspect, and (**c**) roughness. Blue dots in (**a**,**c**) represent 12 glaciers listed in Table 1, and the corresponding blue lines represent their linear fitting. Blue dots in (**b**) represent the 4 large slope glaciers' (ID.7,8,9,10 in Table 1) standard deviation of dh trends.

5.2. Climate Changes

According to the estimated glacier elevation change in this study, we reported that twelve glaciers showed increasing trends of surface elevation while three glaciers were in balance, and the remaining two glaciers showed significant thinning trends. What are the possible causes of the different behaviors of the various glaciers in the area?

First, glacier heterogeneity dynamics are associated with the surging dynamic mechanism discussed in the previous section. Glacier surging causes merely a redistribution of ice mass. When glacier surging occurs, the rapid movement transports the ice mass to the low-altitude zone. Therefore, glacier surging is responsible for the estimated decline in both glaciers of Zhongfeng (ID 6 and ID 11).

Secondly, the glacier changes are related to long-term climatic changes. We collected meteorological data from 1973 to 2020 from the China Meteorological Data Service Centre (https://data.cma.cn, accessed on 29 May 2022) to analyze glacier changes and climate factors. (1) The temperature may be one of the most critical factors controlling the glacier changes. Based on the averaged records from the meteorological stations of the Shijieh, Geze, Minfeng, Hotian, Pishan, and Yutian stations closest to the WKM glacier, it is found

that the summer average air temperature showed significant upward trends before 2000 (Figure 10a). However, variability in the air temperature was not significant after 2000. There was a warming "hiatus" (Figure 10a, and [12,36]), which may be the potential cause of glaciers in balance, such as the three glaciers of ID 1, 9, and 17. 2. The difference in the sensitivity of glaciers to climate change can result in varying glacier responses. The precipitation is another critical factor influencing the glacier variations on the Tibetan Plateau. In contrast to other regions of the QTP, the WKM glaciers are more sensitive to precipitation changes than temperature variability [37]. Especially after 2000, Figure 10b reveals a more significant increase in the annual precipitation resulting from the strengthening westerlies [11]. Therefore, the increasing rainfall may contribute more to the thickening of the twelve glaciers.

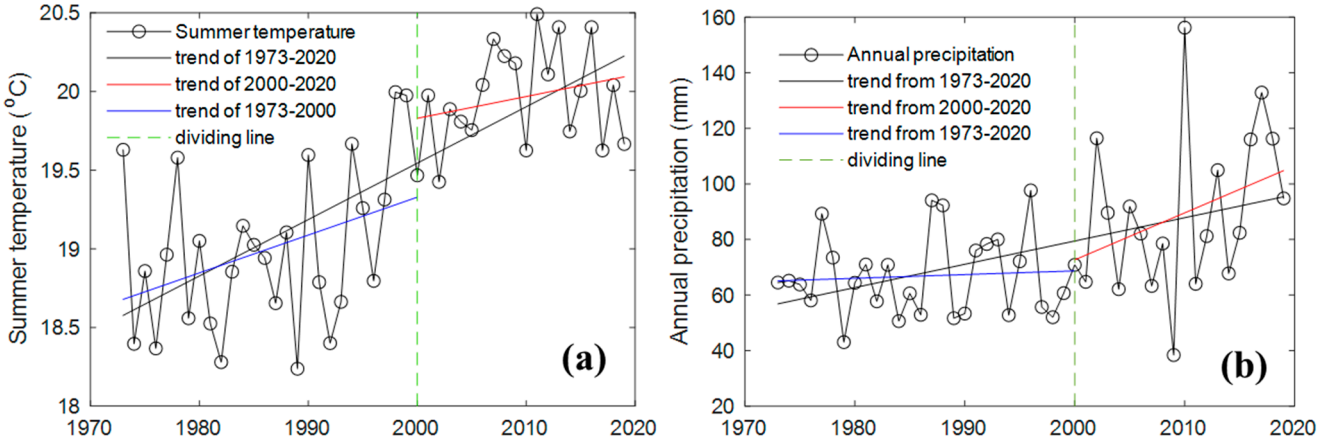

Figure 10. Summer temperature (**a**) and annual precipitation (**b**) changes in the WKM region.

It should be noted that climate change has difficulty fully explaining the multiple fluctuations. An important reason is that the duration of the glacier observations from ICESat is only 6 years (2003~2008) Extending the continuous glacier observations to a longer period (e.g., over 20 years) is necessary to make them consistent with the long-term climatic states. To this end, subsequent ICESat-2 satellites provide this possibility. Current ICESat-2 observations are available for more than 2 years (2019 to present), but there is a 10-year data gap from the last acquisition of ICESat observations. Therefore, this study has not yet introduced ICESat-2 data to analyze glacier changes. In addition, the ICESat footprint covers only part of the WKM glaciers, which may cause a particular bias in the estimated actual mass balance of the entire glacier. ICESat-2 also covers denser footprints over the whole glaciers, and it will be more meaningful for updating solid estimates of glacier change and climate factor analysis.

6. Conclusions

The mass balance of the local glaciers in the Tibetan Plateau plays a key and direct role in the climate response. In this study, the glacier elevation change trends, ice flux divergence, and SMB of entire WKM glaciers were derived using satellite altimetry, glacier velocity, and thickness field datasets. To reduce sensitivity to potential noise and overcome uncertainties, robust linear fitting methods were considered to estimate elevation difference trends. During the period 2003–2008, the SMB of the 17 local glaciers was found to range from -0.39 ± 0.11 to 0.83 ± 0.10 m/a, with an average mass gain of 0.21 ± 0.98 m/a, by combining the ICESat-based surface elevation trend of 0.21 ± 0.14 m/a and ice flux divergence of 0.00 ± 0.97 m/a. However, the ice flux divergence of the ice tongue is more pronounced for individual glaciers due to the more significant gradient of surface velocity and thickness fields. These results show high heterogeneity in glacier dynamics. We found that the terrain-instability-induced glacier surging process may be the most important influencing factor for glacier heterogeneity dynamics. The glacier surging causes the glacial

mass to shift from the high-altitude area to the low-altitude area; it only causes the transfer of material and does not change the mass gain or loss of the glacier. In addition, since 2000, there has been warming hiatus in the air temperature and significantly increased precipitation changes, which may account for the balance and thickening of glaciers.

Author Contributions: Conceptualization, L.G. and X.Y.; methodology, L.G.; software, L.G. and J.Q.; validation, L.G. and W.C.; formal analysis, L.G. and X.Y.; investigation, W.C.; resources, L.G., J.Q. and W.C.; data curation, X.Y.; writing—original draft preparation, L.G., X.Y. and J.Q.; writing—review and editing, L.G., X.Y. and J.Q.; visualization, X.Y.; supervision, X.Y.; project administration, W.C.; funding acquisition, L.G. and X.Y. All authors have read and agreed to the published version of the manuscript.

Funding: This work was supported by the National Natural Science Foundation of China (Grant Nos. 42090044, U2006211), the Marine S&T Fund of Shandong Province for Pilot National Laboratory for Marine Science and Technology (Qingdao) (Grant No. 2022QNLM050301-2), the Natural Science Foundation of Shandong Province, China (Grant No. ZR2021MD022), and the Strategic Priority Research Program of the Chinese Academy of Sciences (Grant Nos. XDA19060101, XDB42000000), Major scientific and technological innovation projects in Shandong Province (Grant No. 2019JZZY010102), the CAS Program (Grant No. Y9KY04101L).

Data Availability Statement: The ICESat/GLAS data are available from http://nsidc.org/ (accessed on 29 May 2022). Digital elevation model is available from https://www.un-spider.org/links-and-resources/data-sources/digital-elevation-model-srtm-3-nasa (accessed on 29 May 2022). The Second Glacier Inventory Dataset of China (Version 1.0, doi:10.3972/glacier.001.2013.db) is available from https://data.tpdc.ac.cn/en/data/f92a4346-a33f-497d-9470-2b357ccb4246/ (accessed on 29 May 2022). The meteorological data are freely available via the website http://data.cma.cn/en (accessed on 29 May 2022). The surface velocity field is freely available via the NASA MEaSUREs project at the website https://its-live.jpl.nasa.gov/ (accessed on 29 May 2022), and the glacier thickness field is freely available at https://doi.org/10.3929/ethz-b-000315707 (accessed on 29 May 2022).

Acknowledgments: The authors are very grateful to Baotian Pan and Bo Cao at College of Earth and Environmental Sciences, Lanzhou University, Lanzhou, China for providing the advice on the interaction of glaciers with climatic factors.

Conflicts of Interest: The authors declare no conflict of interest.

References

1. Immerzeel, W.W.; Van Beek, L.P.H.; Bierkens, M.F.P. Climate change will affect the Asian water towers. *Science* **2010**, *328*, 1382–1385. [CrossRef]
2. Jacob, T.; Wahr, J.; Pfeffer, W.T.; Swenson, S. Recent contributions of glaciers and ice caps to sea level rise. *Nature* **2012**, *482*, 514–518. [CrossRef] [PubMed]
3. Wingham, D.J.; Ridout, A.J.; Scharroo, R.; Arthern, R.J.; Shum, C.K. Antarctic elevation change from 1992 to 1996. *Science* **1998**, *282*, 456–458. [CrossRef]
4. Johannessen, O.M.; Khvorostovsky, K.; Miles, M.W.; Bobylev, L.P. Recent icesheet growth in the interior of Greenland. *Science* **2005**, *310*, 1013–1016. [CrossRef] [PubMed]
5. Magruder, L.A.; Webb, C.E.; Urban, T.J.; Silverberg, E.C.; Schutz, B.E. ICESat altimetry data product verification at White Sands Space Harbor. *IEEE Trans. Geosci. Remote Sens.* **2007**, *45*, 147–155. [CrossRef]
6. Kääb, A. Glacier volume changes using ASTER satellite stereo and ICESat GLAS laser altimetry. A test study on EdgeØya, Eastern Savalbard. *IEEE Trans. Geosci. Remote Sens.* **2008**, *46*, 2823–2830. [CrossRef]
7. Kääb, A.; Berthier, E.; Nuth, C.; Gardelle, J.; Arnaud, Y. Contrasting patterns of early twenty-first-century glacier mass change in the Himalayas. *Nature* **2012**, *488*, 495–498. [CrossRef]
8. Gardner, A.S.; Moholdt, G.; Cogley, J.G.; Wouters, B.; Arendt, A.A.; Wahr, J.; Berthier, E.; Hock, R.; Pfeffer, W.T.; Kaser, G.; et al. A Reconciled Estimate of Glacier Contributions to Sea Level Rise: 2003 to 2009. *Science* **2013**, *340*, 852–857. [CrossRef]
9. Bolch, T.; Kulkarni, A.; Kääb, A.; Huggel, C.; Paul, F.; Cogley, J.G.; Frey, H.; Kargel, J.S.; Fujita, K.; Scheel, M.; et al. The State and Fate of Himalayan Glaciers. *Science* **2012**, *336*, 310–314. [CrossRef]
10. Bolch, T.; Shea, J.M.; Liu, S.; Azam, F.M.; Gao, Y.; Gruber, S.; Immerzeel, W.W.; Kulkarni, A.; Li, H.; Tahir, A.A.; et al. Status and Change of the Cryosphere in the Extended Hindu Kush Himalaya Region. In *The Hindu Kush Himalaya Assessment*; Wester, P., Mishra, A., Mukherji, A., Shrestha, A., Eds.; Springer: Cham, Switzerland, 2019; pp. 209–255. [CrossRef]
11. Yao, T.; Thompson, L.; Yang, W.; Yu, W.; Gao, Y.; Guo, X.; Yang, X.; Duan, K.; Zhao, H.; Xu, B.; et al. Different glacier status with atmospheric circulations in Tibetan Plateau and surroundings. *Nat. Clim. Chang.* **2012**, *2*, 663–667. [CrossRef]

12. Wang, Y.; Hou, S.; Huai, B.; An, W.; Pang, H.; Liu, Y. Glacier anomaly over the western Kunlun Mountains, Northwestern Tibetan Plateau, since the 1970s. *J. Glaciol.* **2018**, *64*, 624–636. [CrossRef]
13. Huang, M. The climatic conditions of polar-type glaciers development in china. *Chin. Geogr. Sci.* **1995**, *5*, 97–103. [CrossRef]
14. Shen, Y. *An Overview of Glaciers, Retreating Glaciers and Their Impact in the Tibetan Plateau*; Cold and Arid Regions Environmental and Engineering Research Institute (CAREERI), Chinese Academy of Sciences (CAS): Lanzhou, China, 2004.
15. Brun, F.; Wagnon, P.; Berthier, E.; Shea, J.M.; Immerzeel, W.W.; Kraaijenbrink, P.D.A.; Vincent, C.; Reverchon, C.; Shrestha, D.; Arnaud, Y. Ice cliff contribution to the tongue-wide ablation of Changri Nup Glacier, Nepal, central Himalaya. *Cryosphere* **2018**, *12*, 3439–3457. [CrossRef]
16. Bisset, R.R.; Dehecq, A.; Goldberg, D.N.; Huss, M.; Bingham, R.G.; Gourmelen, N. Reversed Surface-Mass-Balance Gradients on Himalayan Debris-Covered Glaciers Inferred from Remote Sensing. *Remote Sens.* **2020**, *12*, 1563. [CrossRef]
17. Wagnon, P.; Brun, F.; Khadka, A.; Berthier, E.; Shrestha, D.; Vincent, C.; Arnaud, Y.; Six, D.; Dehecq, A.; Ménégoz, M.; et al. Reanalysing the 2007–19 glaciological mass-balance series of Mera Glacier, Nepal, Central Himalaya, using geodetic mass balance. *J. Glaciol.* **2021**, *67*, 117–125. [CrossRef]
18. Miles, E.; McCarthy, M.; Dehecq, A.; Kneib, M.; Fugger, S.; Pellicciotti, F. Health and sustainability of glaciers in High Mountain Asia. *Nat. Commun.* **2021**, *12*, 2868. [CrossRef]
19. Zemp, M.; Thibert, E.; Huss, M.; Stumm, D.; Denby, C.R.; Nuth, C.; Nussbaumer, S.U.; Moholdt, G.; Mercer, A.; Mayer, C.; et al. Uncertainties and re-analysis of glacier mass balance measurements Uncertainties and re-analysis of glacier mass balance measurements. *Cryosphere Discuss.* **2013**, *7*, 789–839. [CrossRef]
20. Van Tricht, L.; Huybrechts, P.; Van Breedam, J.; Vanhulle, A.; Van Oost, K.; Zekollari, H. Estimating surface mass balance patterns from unoccupied aerial vehicle measurements in the ablation area of the Morteratsch–Pers glacier complex (Switzerland). *Cryosphere* **2021**, *15*, 4445–4464. [CrossRef]
21. Bhang, K.J.; Schwartz, F.W.; Braun, A. Verification of the vertical error in C-band SRTM DEM using ICESat and Landsat-7, Otter Tail County, MN. *IEEE Trans. Geosc. Remote Sens.* **2007**, *45*, 36–44. [CrossRef]
22. Neckel, N.; Kropacek, J.; Bolch, T.; Hochschild, V. Glacier mass changes on the Tibetan Plateau 2003–2009 derived from ICESat laser altimetry measurements. *Environ. Res. Lett.* **2014**, *9*, 014009. [CrossRef]
23. Wang, Y.; Li, J.; Wu, L.; Guo, L.; Hu, J.; Zhang, X. Estimating the Changes in Glaciers and Glacial Lakes in the Xixabangma Massif, Central Himalayas, between 1974 and 2018 from Multisource Remote Sensing Data. *Remote Sens.* **2021**, *13*, 3903. [CrossRef]
24. Guo, W.; Liu, S.; Yao, X.; Xu, J.; Shangguan, D.; Wu, L.; Zhao, J.; Liu, Q.; Jiang, Z.; Wei, J.; et al. *The Second Glacier Inventory Dataset of China (Version 1.0)*; Cold and Arid Regions Science Data Center: Lanzhou, China, 2014. [CrossRef]
25. Farinotti, D.; Huss, M.; Fürst, J.J.; Landmann, J.; Machguth, H.; Maussion, F.; Pandit, A. A consensus estimate for the ice thickness distribution of all glaciers on Earth. *Nat. Geosci.* **2019**, *12*, 168–173. [CrossRef]
26. Kääb, A.; Treichler, D.; Nuth, C.; Berthier, E. Brief communication: Contending estimates of 2003–2008 glacier mass balance over the Pamir–Karakoram–Himalaya. *Cryosphere* **2015**, *9*, 557–564. [CrossRef]
27. Ke, L.; Ding, X.; Song, C. Heterogeneous changes of glaciers over the western Kunlun Mountains based on ICESat and Landsat-8 derived glacier inventory. *Remote Sens. Environ.* **2015**, *168*, 13–23. [CrossRef]
28. Zhang, J.; Fu, B.H.; Wang, L.M.; Maimaiti, A.; Ma, Y.X.; Yan, F. Glacier Changes in the West Kunlun Mountains Revealed by Landsat Data from 1994 to 2016. *IOP Conf. Ser. Earth Environ. Sci.* **2017**, *74*, 012002. [CrossRef]
29. Jansson, P. Effect of uncertainties in measured variables on the calculated mass balance of Storglaciären. *Geogr. Ann. Ser. A Phys. Geogr.* **1999**, *81*, 633–642. [CrossRef]
30. Bao, W.; Liu, S.; Wei, J.; Guo, W. Glacier changes during the past 40 years in the West Kunlun Shan. *J. Mt. Sci.* **2015**, *12*, 344–357. [CrossRef]
31. Yasuda, T.; Furuya, M. Short-term glacier velocity changes at West Kunlun Shan, Northwest Tibet, detected by Synthetic Aperture Radar data. *Remote Sens. Environ.* **2013**, *128*, 87–106. [CrossRef]
32. Chen, W.; Yao, T.; Zhang, G.; Li, F.; Zheng, G.; Zhou, Y.; Xu, F. Towards ice-thickness inversion: An evaluation of global digital elevation models (DEMs) in the glacierized Tibetan Plateau. *Cryosphere* **2022**, *16*, 197–218. [CrossRef]
33. Millan, R.; Mouginot, J.; Rabatel, A.; Morlighem, M. Ice velocity and thickness of the world's glaciers. *Nat. Geosci.* **2022**, *15*, 124–129. [CrossRef]
34. Li, C.; Yang, T.; Tian, H. Variation of West Kunlun Mountains glacier during 1990–2011. *Prog. Geogr.* **2013**, *32*, 548–559. (In Chinese)
35. Cao, B.; Guan, W.; Li, K.; Wen, Z.; Han, H.; Pan, B. Area and Mass Changes of Glaciers in the West Kunlun Mountains Based on the Analysis of Multi-Temporal Remote Sensing Images and DEMs from 1970 to 2018. *Remote Sens.* **2020**, *12*, 2632. [CrossRef]
36. Wang, Y.; Hou, S.; An, W.; Pang, H.; Liu, Y. Slight glacier reduction over the northwestern Tibetan Plateau despite significant recent warming. *Cryosphere Discuss.* **2016**. [CrossRef]
37. Kapnick, S.B.; Delworth, T.L.; Ashfaq, M.; Malyshev, S.; Milly, P.C.D. Snowfall less sensitive to warming in Karakoram than in Himalayas due to a unique seasonal cycle. *Nat. Geosci.* **2014**, *7*, 834–840. [CrossRef]